

# Photometry and spectroscopy of the newly discovered eclipsing binary GSC 4589-2999

A.Liakos<sup>1,\*</sup>, P.Bonfini<sup>2,3</sup>, P.Niarchos<sup>1</sup>, and D.Hatzidimitriou<sup>1,3</sup>

<sup>1</sup> Department of Astrophysics, Astronomy and Mechanics, University of Athens, GR 157 84, Zografos, Athens, Hellas

<sup>2</sup> Department of Physics, University of Crete, PO Box 2208, 71003, Heraklion, Hellas

<sup>3</sup> IESL, Foundation for Research and Technology-Hellas, 71110, Heraklion, Hellas

Received 30 May 2005, accepted 11 Nov 2005

Published online later

**Key words** stars: binaries: eclipsing – stars: fundamental parameters – stars: individual (GSC 4589-2999) – techniques: photometric – techniques: spectroscopic

New CCD light curves of the recently detected eclipsing variable GSC 4589-2999 were obtained and analysed using the Wilson-Deninney code. Spectroscopic observations of the system allowed the spectral classification of the components and the determination of their radial velocities. The physical properties and absolute parameters of the components and an updated ephemeris of the system are given.

© 2006 WILEY-VCH Verlag GmbH & Co. KGaA, Weinheim

## 1 Introduction and Observations

Eclipsing binary systems offer unique conditions to measure fundamental parameters of stars, such as stellar masses, radii and luminosities, which are of great importance in studies of stellar structure and evolution.

Using extensive photometric and spectroscopic data, we performed a comprehensive study of the newly discovered eclipsing system GSC 4589-2999 (=TYC 4589-2999-1,  $\alpha_{2000} = 20^h 15^m 0.2^s$ ,  $\delta_{2000} = +76^\circ 54' 18.2''$ ,  $V=10.6$  mag). The light variability report (as a by-product of observations of the eclipsing system EG Cep), the first light curves and ephemeris of the system were published by Liakos & Niarchos (2007).

The new photometric observations of the system were carried out at the Gerostathopoulion Observatory of the University of Athens, during 44 nights in June–October 2007 and 12 nights in June–July 2008, using the 0.4m Cassegrain telescope equipped with the ST-8XMEI CCD camera and the BVRI Bessell photometric filters.

The spectroscopic observations were obtained with the 1.3m Ritchey–Cretien telescope equipped with a 2000×800 ISA SITE CCD camera at Skinakas Observatory, located on the island of Crete, Hellas, on September 2007, September 2008 and May 2009. For the spectral classification, we used the Low Resolution Spectrograph which is incorporated in the Focal Reducer instrument. For the spectral classification we used a reflection grating of 1302 lines/mm giving a nominal dispersion of 1.04 Å/pixel, and an appropriate wavelength coverage (see Table 2) to include both H $\alpha$  and H $\beta$  Balmer lines. For the radial velocity (hereafter RVs) mea-

**Table 1** The photometric comparison and check stars. The magnitudes information are given in The Tycho-2 Catalogue (Høg 2000)

Star	B <sub>TYC</sub>	V <sub>TYC</sub>	remarks
GSC 4589-2999	11.33 (6)	10.61 (4)	variable
GSC 4589-2984	11.86 (8)	10.93 (6)	comparison
GSC 4589-2842	13.4 (3)	11.6 (1)	check

surements a 2400 lines/mm grating was used, giving a nominal dispersion of 0.55 Å/pixel, while the wavelength range was selected to include the Mg I triplet and other metallic lines.

## 2 Data reduction

### 2.1 Photometry

Differential magnitudes were obtained using the software *MuniWin* v.1.1.23 (Hroch 1998). The magnitudes have not been transformed to a standard system and the colour extinction was not taken into account since standard star observations were not performed. Information about the comparison stars can be found in Table 1.

### 2.2 Spectroscopy

Various exposure times for the observations of 2007, 2008, 2009 were used (for details see Table 2). Before and after each on-target observation, an arc calibration exposure (Ne-HeAr) was recorded. Arc spectra were extracted from the arc exposures by applying exactly the same profiles as to the corresponding object spectra and they were used to calibrate the object spectra.

\* Corresponding author: e-mail: alliakos@phys.uoa.gr

**Table 2** The spectroscopic observations log

Date of observation	UT	Phase	Exposure time (sec)	Wavelength coverage (Å)
29-9-2007	17:36	0.544	300	4728-6828
29-9-2007	17:42	0.547	300	4728-6828
29-9-2007	19:28	0.590	300	4728-6828
29-9-2007	19:35	0.593	300	4728-6828
3-9-2008	01:44	0.497	600	4713-6792
12-5-2009	23:54	0.688	1800	4535-5621
13-5-2009	21:19	0.216	1800	4535-5621
14-5-2009	20:09	0.780	1800	4535-5621
14-5-2009	20:49	0.795	1800	4535-5621

For the spectral classification procedure, a total of 44 standards of spectral types ranging from O8 to M6 were observed with an identical instrument configuration as the targets: 15 were observed on September 29, 2007, 14 were observed on 31 August 2008 and another 15 were taken from Hatzidimitriou et al. (2006). All standard star spectra were reduced and calibrated in exactly the same way as the targets, following the procedure described in the following. The data reduction was performed using the *IRAF* package 2.13-BETA2 (2006). The frames were bias subtracted and the sky background was removed. The spectra were subsequently traced and extracted using the all-in-one subpackage *apextract*.

For the determination of the RVs, the softwares *Radial Velocity reductions* v.2.1d (Nelson 2009) and *Broadening Functions* v.2.4c (Nelson 2009) were used.

### 3 Data analysis

#### 3.1 Spectroscopic analysis

On September 2007 the spectra were obtained on the rising branch of the secondary minimum, and particularly the second set of spectra includes the spectra of both stars. On September 2008 the spectroscopic observations were obtained during the total eclipse, thus obtaining a clear spectrum for the primary (larger, hotter and more massive) component. The exact phase moments when the spectra were taken are given in Table 2. The spectrum of the secondary component was obtained by the subtraction of the two spectra (the spectra of 2008 from those of 2007), after normalizing them to the same continuum, line-free point. The resulting spectrum is of quite high signal-to-noise and clearly indicates a cooler star (see Fig. 1b), as it will be discussed below.

The classification of the spectra was achieved in two steps:

(i) Cross-correlation with the 44 standard star spectra, using the method described in detail in Hatzidimitriou et al. (2006). The accuracy of the spectral classification achieved with this method depends on the fineness of the grid of standard spectra used and on the signal-to-noise ratio of the

**Table 3** The heliocentric radial velocities measurements

HJD - 2450000	Phase	V <sub>1</sub> (Km/sec)	V <sub>2</sub> (Km/sec)
4964.5048	0.688	51 (29)	-165 (17)
4965.3971	0.216	-93 (24)	156 (29)
4966.3490	0.780	57 (24)	-180 (18)
4966.3747	0.795	71 (32)	-170 (16)

cross-correlated spectra, and it is found to be around 0.3-0.4 of a spectral type (cf. Bonfini et al. 2009).

(ii) Visual detailed comparison of spectral features with standard spectra around the spectral type indicated by step (i). This procedure required prior normalization of the continua of the spectra, and leads to a confirmation and fine-tuning of the cross-correlation result.

Using steps (i) and (ii), we estimate that the primary component of the system, namely GSC 4589-2999a (spectrum obtained in September 2008), is of spectral type G1.5 ±0.5. The spectrum is shown in Fig. 1a (solid black line), along with the spectrum of the G2 standard star HD 196755 and of the G0 standard SF-18, for comparison. The spectrum of the secondary component, GSC 4589-2999b, resulted from the subtraction of the spectra taken in 2007 and 2008, is of K4 type, with an uncertainty of one subclass. The spectrum is shown in Fig. 1b together with the comparison spectra of the K4 star HD 198550 and the K5 star 32 Vul. The cross correlation diagrams for each component are overlotted in Fig. 1c.

For the RVs determination, the Broadening Functions (hereafter BFs) method (Rucinski 2002) on the spectra of 2009 was used. We cropped all spectra in order to avoid the broad H<sub>β</sub> line, and we included all the sharp metallic lines between 4865-5355 Å. Each RV value and its error was derived statistically (mean value and error) from the respective velocities resulted from BFs method by using different standard stars. The standard stars were HIP 40497, HIP 61317, HIP 65721 which are of F7, G0 and G5 spectral type, respectively. The heliocentric RVs with their errors in parentheses are given in Table 3, and the RVs plot is illustrated in Fig. 5.

#### 3.2 Photometric and radial velocity analysis

The updated ephemeris of the system was calculated by applying the least squares method on all the available minima timings (Liakos & Niarchos 2009) and it is given by the following relation:

$$\text{Min.I}=\text{HJD } 2454642.4992(2)+1.688653(1)^d \times \text{E}$$

The light curves and the RVs curves were analyzed with the *PHOEBE* v.0.29d software (Prša & Zwitter 2005), which uses the 2003 version of the Wilson-Devinney code (Wilson & Devinney 1971; Wilson 1979, 1990). The code was applied in MODE 2 (detached system) and all light (BVRI) and RV curves were analysed simultaneously.

The temperature of the primary  $T_1$  was fixed to the typical value of a G1.5 star, namely 5830 K, while the tem-

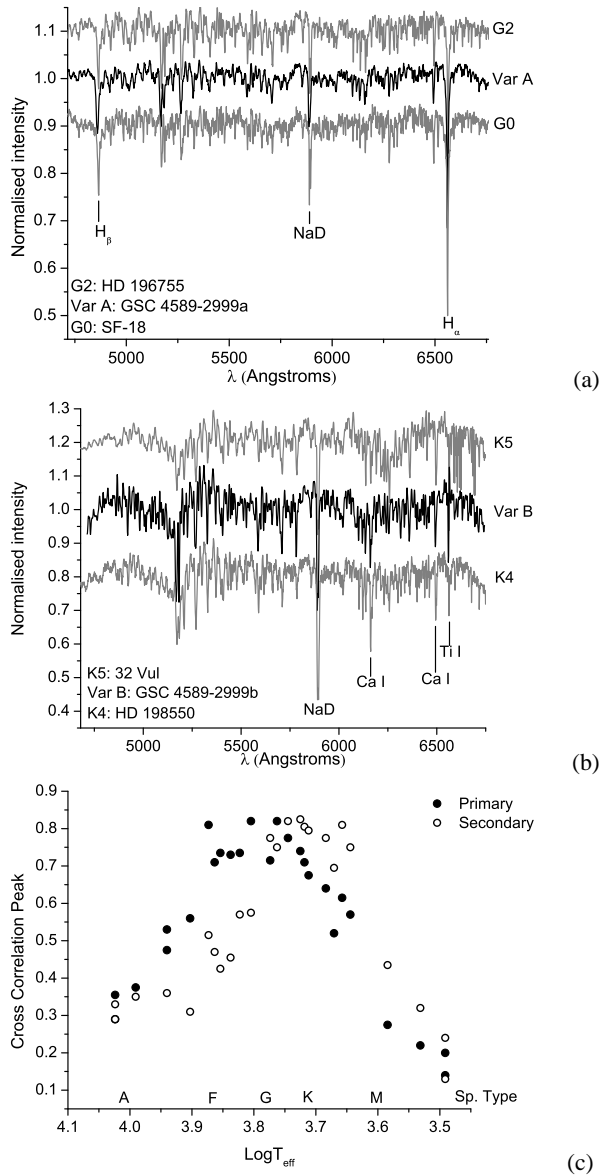


**Fig. 1** The spectra of the primary (a) and secondary (b) components of GSC 4589-2999. Information about the standard stars are given in the text. (c) The Cross Correlation plots for each component of the system.

perature of the secondary  $T_2$  was given initially the value 4550 K, a typical value for a K4 star, but during the iterations it was left as free parameter. Given the spectroscopic error of the primary's spectral type (see section 3.1), its corresponding temperature has an accuracy of 40 K. Hence, the error of the  $T_2$  value was calculated according to the error propagation method. The albedo of each component, namely  $A_1$  and  $A_2$ , and the gravity darkening coefficients,  $g_1$  and  $g_2$ , were assigned theoretical values, according to the spectral types of the components. The values of limb darkening coefficients,  $x_1$  and  $x_2$ , were taken from the tables of van Hamme (1993). The dimensionless potentials  $\Omega_1$  and  $\Omega_2$ , the mass ratio  $q$ , the fractional luminosity  $L_1$  of the primary component, the systemic radial velocity  $V_0$ , the semi

**Table 4** The parameters (par.) of GSC 4589-2999 derived from the light and radial velocities curves solution. P denotes the primary and S the secondary component, respectively. The errors are given in parentheses and correspond to the last digit of each value.

Parameter	Value	Parameter	Value
$i$ (deg)	86.3 (2)	$x_{1,B}$	0.731
$q$ ( $m_2/m_1$ )	0.46 (3)	$x_{2,B}$	0.898
$a$ ( $R_\odot$ )	8.3 (3)	$x_{1,V}$	0.597
$K_1$ (km/sec)	78 (3)	$x_{2,V}$	0.758
$K_2$ (km/sec)	169 (1)	$x_{1,R}$	0.514
$V_0$ (km/sec)	-13 (3)	$x_{2,R}$	0.658
$T_1$ (K)	5830 (40)	$x_{1,I}$	0.434
$T_2$ (K)	4616 (116)	$x_{2,I}$	0.549
$\Omega_1$	4.59 (1)	<u>Spot</u>	
$\Omega_2$	5.75 (2)	Co-lat (deg)	86 (6)
$L_1/(L_1+L_2)_B$	0.961 (1)	Co-lon (deg)	44 (2)
$L_1/(L_1+L_2)_V$	0.949 (1)	R (deg)	20 (6)
$L_1/(L_1+L_2)_R$	0.940 (1)	$T_{spot}/T_{sur}$	0.6 (2)
$L_1/(L_1+L_2)_I$	0.929 (1)	<u>Fractional radii</u>	
$L_2/(L_1+L_2)_B$	0.039 (1)	$r_1$ (pole)	0.24
$L_2/(L_1+L_2)_V$	0.051 (1)	$r_1$ (point)	0.25
$L_2/(L_1+L_2)_R$	0.060 (1)	$r_1$ (side)	0.24
$L_2/(L_1+L_2)_I$	0.071 (1)	$r_1$ (back)	0.25
$g_1$	0.32	$r_2$ (pole)	0.10
$g_2$	0.32	$r_2$ (point)	0.10
$A_1$	0.5	$r_2$ (side)	0.10
$A_2$	0.5	$r_2$ (back)	0.10

major axis  $a$  and the inclination of the system's orbit  $i$  were treated as adjustable parameters. Due to asymmetries near the primary maxima of the light curves, a cool spot on the surface of the cooler component was assumed and its parameters (latitude  $Co - lat$ , longitude  $Co - lon$ , radius  $R$  and temperature factor  $T_{spot}/T_{sur}$ ) were also adjusted. Another analysis without the cool spot was also performed, but the result was worse. The spotted solution resulted in a sum of squared residuals  $\sum x^2=0.0032$ , while the unspotted one yielded to a value of 0.0059, therefore we chose to adopt the spotted solution. The comparison between the models including or not the spot is presented in Fig. 3. The maximum radial velocity of each component, namely  $K_1$  and  $K_2$ , was calculated by fitting a sinusoidal function on the points of each RV curve. The synthetic and observed light and RV curves are shown in Figs 2 and 5, respectively, the 3D representation is illustrated in Fig. 4, and the derived parameters are listed in Table 4.

#### 4 Absolute elements of the components

The geometric and photometric elements, derived from the simultaneous analysis of the light and RV curves, were used to compute the absolute elements of the components. These elements, listed in Table 5, are used to place the two components on the Mass-Radius (M-R) diagram (Fig. 6) in order to examine their evolutionary status.

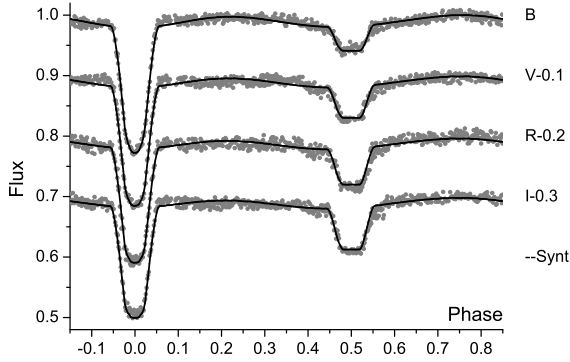


**Fig. 2** Synthetic (solid lines) and observed (points) light curves of GSC 4589-2999.

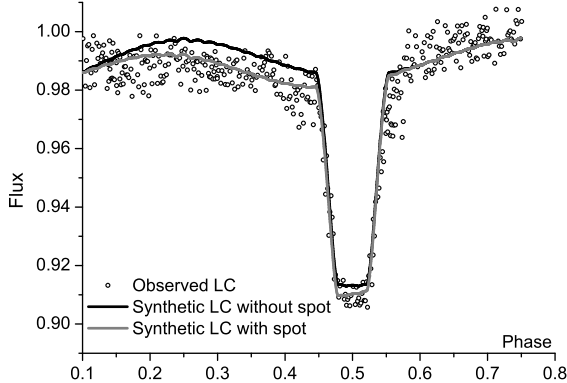


**Fig. 3** The comparison between the fit on the data points of the synthetic light curves in I filter for spotted (grey solid line) and unspotted (black solid line) models.

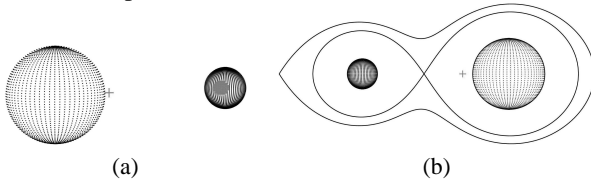


**Fig. 4** The 3D model of GSC 4589-2999 at the phases: (a) 0.34 where the cool spot is indicated and (b) 0.75 where the center of mass (+) and inner and outer Roche Lobes are shown.

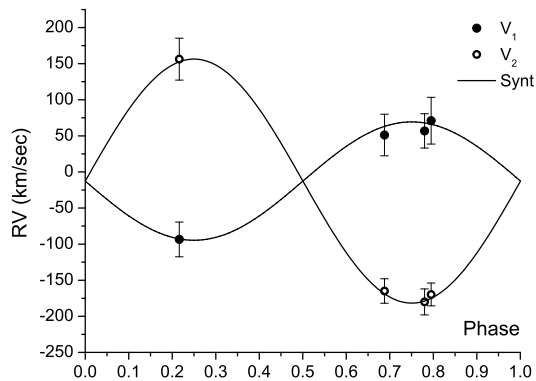


**Fig. 5** Synthetic (solid lines) and observed (points) radial velocity curves of GSC 4589-2999.

**Table 5** The absolute elements of the components (P: Primary, S: Secondary). The errors are given in parentheses.

	M ( $M_{\odot}$ )	R ( $R_{\odot}$ )	$T_{eff}$ (K)	L ( $L_{\odot}$ )	$M_{bol}$ (mag)
P	1.8 (1)	2.02 (4)	5830 (40)	4.2 (2)	3.2 (3)
S	0.8 (1)	0.85 (2)	4616 (116)	0.3 (1)	6.1 (8)

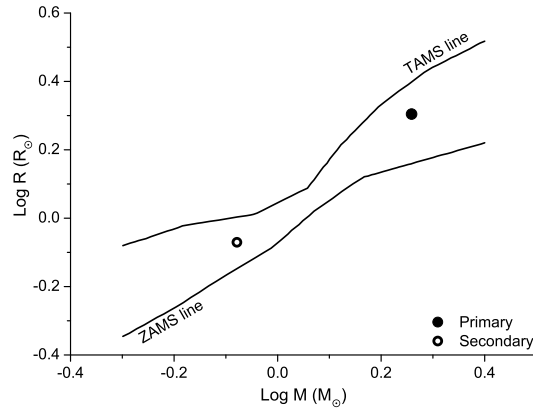


**Fig. 6** The position of the components of GSC 4589-2999 in the M-R diagram.

Both components lie inside the Terminal Age Main Sequence (TAMS) and Zero Age Main Sequence (ZAMS) limits, revealing their Main-Sequence (MS) nature. However, the primary component is closer to TAMS line, while the secondary one is almost in the middle of the limits. This result is in agreement with the theory of stellar evolution according to their initial mass, since the more massive component is found to be more evolved than the secondary, assuming a simultaneous birth.

## 5 Discussion and conclusions

The main contribution of the present paper is the first determination of the physical parameters of the newly discovered eclipsing binary system GSC 4589-2999. This study is based on high-quality spectroscopic and multicolour CCD observations.

The two components of the system are classified as G1.5  $\pm$  0.5 (primary) and K4  $\pm$  1 (secondary), respectively. The light curve analysis yielded a temperature of the secondary component as 4616 K, in very good agreement, within the error limit, with the temperature corresponding to the spectral type (K3/5, 4685 K - 4415 K), derived from our spectroscopic observations.

The shape of the light curves indicates an Algol-type eclipsing binary with a period close to 1.69 d. A simultaneous analysis of the light and radial velocity curves resulted in a detached configuration with zero eccentricity. A small asymmetry near the primary maximum was better explained by assuming a cool spot on the surface of the secondary component, but it is well known that spot solution suffers from non-uniqueness.

The derived absolute elements were used to study the evolutionary status of the two components. It was found that both components belong to the MS, while the primary component (more massive and hotter) is more evolved than the secondary.

*Acknowledgements.* This work has been financially supported by the Special Account for Research Grants No 70/4/9709 of the National & Kapodistrian University of Athens, Hellas. We thank P. Reig for the spectroscopic observations of September of 2008. Part of the work presented here was done while P. Bonfini was still a student at the University degli Studi di Milano - Bicocca, Italy and was possible thanks to the Erasmus Program. Skinakas Observatory is a collaborative project of the University of Crete, and the Foundation for Research and Technology-Hellas.

## References

- Bonfini, P., Hatzidimitriou, D., Pietsch, W., Reig, P.: 2009, A&A 507, 705
- Hatzidimitriou, D., Pietsch, W., Misanovic, Z., Rieg, R., Haberl, F.: 2006, A&A 451, 835
- Høg, F.: 2000, Encyclopedia of Astronomy and Astrophysics, Edited by Paul Murdin, article 2862. Bristol: Institute of Physics Publishing, 2001
- Hroch, F.: 1998, Proceedings of the 29th Conference on Variable Star Research 30
- Liakos, A. & Niarchos, P.: 2007, IBVS 5900, 2
- Liakos, A. & Niarchos, P.: 2009, IBVS 5897, 1
- Nelson, R. H.: 2009, Software by Bob Nelson  
<http://members.shaw.ca/bob.nelson/software1.htm>
- Prša, A. & Zwitter, T.: 2005, ApJ 628, 426
- Rucinski, S.: 2002, AJ 124, 1746
- van Hamme, W.: 1993, AJ 106, 2096
- Wilson, R.E. & Devinney, E.J.: 1971, ApJ 166, 605
- Wilson, R.E.: 1979, ApJ 234, 1054
- Wilson, R.E.: 1990, ApJ 356, 613